Available online at www.sciencedirect.com
SCIENCE DIRECT®
Journal of Electroanalytical Chemistry 567 (2004) 331–338
Journal of Electroanalytical Chemistry
www.elsevier.com/locate/jelechem

Catalytic oxidation of nitric oxide and nitrite mediated by water-soluble high-valent iron porphyrins at an ITO electrode

Jianping Lei [a], Huangxian Ju [b], Osamu Ikeda [a,*]

[a] Department of Chemistry, Faculty of Science, Kanazawa University, General Education Hall, Kakuma, Kanazawa, Ishikawa 920-1192, Japan
[b] State Key Laboratory of Coordination Chemistry, Department of Chemistry, Institute of Chemical Biology, Nanjing University, Nanjing 210093, PR China

Received 16 May 2003; received in revised form 29 September 2003; accepted 12 December 2003
Available online 10 March 2004

Abstract

A stepwise catalytic oxidation for nitric oxide and nitrite by water-soluble iron(III) meso-tetrakis(*N*-methylpyridinium-4-yl)porphyrin (Fe^{III}(4-TMPyP)) was first revealed by using an ITO electrode. Electrochemical and spectroelectrochemical studies characterized the formation of oxoiron(IV) porphyrin and oxoiron(IV) porphyrin π-cation radical in the oxidation of Fe^{III}(4-TMPyP). O=Fe^{IV}(4-TMPyP) showed selective catalytic oxidation towards NO against NO_2^- with a normalized catalytic current of 3.4. The electrogenerated O=Fe^{IV}(4-TMPyP) π-cation radical effectively catalyzed the oxidation of NO_2^- to NO_3^- via nitrogen dioxide ($^{\cdot}NO_2$) intermediate. Product analysis clarified that nitrite was the sole product in the catalytic oxidation of NO by O=Fe^{IV}(4-TMPyP) electrogenerated at 0.85 V vs. Ag|AgCl, but nitrate was the final product after electrolysis at 1.1 V vs. Ag|AgCl. The different chemical reactivities of high-valent iron porphyrins electrogenerated at the separated potentials indicated the possibility of selective electrochemical detection of NO. A mechanism of typical chemical catalysis was proposed for the catalytic oxidations of NO and NO_2^- by oxoiron(IV) porphyrin complexes.

Keywords: Nitric oxide; Nitrite; Catalytic oxidation; High-valent iron porphyrin; ITO electrode

1. Introduction

It is well known that nitric oxide (NO) plays a significant role as a cell-signal molecule, anti-infective agent, and an antioxidant in many biological processes [1–4]. Measurement of NO in vivo is important but very difficult because of its low concentration and short lifetime. One of the most promising methods is to improve the redox response of NO by using metalloporphyrins and metalloproteins as catalysts. Therefore, it becomes essential to explore the catalytic action between metalloporphyrin and NO. Most of the former research has been focused on the catalytic reduction mechanism of NO [5–8]. Much less attention has been given to the mechanism of the NO oxidation: Malinski et al. [9,10] proposed that nickel porphyrin could act as a catalyst for the oxidation of NO, because of the shift of the NO oxidation potential from +0.9 to +0.65 V. However the interaction between nickel porphyrin film and NO was not obvious. Some other preliminary studies [11,12] suggest that nickel porphyrin modified on the electrode surface acts as a simple organic layer without any specific chemical interaction with NO. Our previous work reported that trace amount of alcohols in Nafion® film might play an important role in the catalytic cycle of NO oxidation on CoTPP [13]. In that sense, the catalytic oxidation mechanism of NO remains poorly understood.

Recently, it has been shown that ferric porphyrin is oxidized into oxoiron(IV) porphyrin (so-called Compound II) and oxoiron(IV) porphyrin π-cation radical (so-called Compound I) via one-electron and two-electron oxidation by chemical oxidants [14,15] or the direct electrochemical oxidation [16–19]. Oxoiron(IV) porphyrins are strong oxidants which can promote

* Corresponding author. Fax: +81-76-264-5988.
E-mail address: osamu@kenroku.kanazawa-u.ac.jp (O. Ikeda).

0022-0728/$ - see front matter © 2004 Elsevier B.V. All rights reserved.
doi:10.1016/j.jelechem.2003.12.041

oxidation, peroxidation, and epoxidation of various biomolecules in vitro [20,21]. Oxoiron(IV) porphyrins have also been utilized to catalyze mono-oxygenation in many chemical reactions including catalytic oxidation of organic substrates [22,23]. O=Fe^{IV}(4-TMPyP) has been shown to catalyze the oxidation of sulfite anion [24]. The reduction of oxoiron(IV) myoglobin or oxoiron(IV) hemoglobin by nitric oxide has been considered as a protective process against oxoiron(IV) hemoprotein-induced oxidations [25]. Several types of Compound II exhibit different rate constants for the reaction of NO with the oxoiron(IV) form, the proximity of positive charges to porphyrin peripheries causes a strong electron-withdrawing effect on the metal sites [26,27] and seems to stabilize oxoiron(IV) species. In this work, we chose Fe^{III}(4-TMPyP) with positive charges at the peripheries as a catalyst to study the interaction between NO and the oxoiron(IV) form.

On the other hand, Compound I has been demonstrated to possess stronger reactivity than Compound II because its redox potential is higher than that of compound II [28]. It has been reported that NO_2^- can be oxidized by heme peroxidases such as HRP, MPO, and LPO in the presence of hydrogen peroxide, most likely to generate nitrogen dioxide as an intermediate. Formation of such a reactive intermediate via Compound I in the catalytic oxidation of NO_2^- also represents an important mechanism contributing to NO-mediated toxicity [29,30]. O=Fe^{IV}(4-TMPyP) and O=Fe^{IV}(4-TMPyP) π-cation radical have been suggested as the intermediates in catalytic decomposition of peroxynitrite by Fe^{III}(4-TMPyP) [31]. Moreover, there is a strong driving force in the thermodynamic feasibility for the oxidation of NO_2^- by compound I, because the NO_2^-/NO_2 potential is well placed between the one-electron oxidation potential of Fe^{IV}P/Fe^{III}P and Fe^{IV}P π-cation radical/Fe^{IV}P [32].

In this paper, we report a stepwise chemical catalysis by high-valent iron porphyrins (4-TMPyP) for nitric oxide and nitrite oxidation at an ITO electrode.

2. Experimental

2.1. Chemicals

Fe^{III}(4-TMPyP) was prepared according to the methods of Pasternack et al. [33] and Bedioui et al. [34]. The product was purified by chromatography with the help of an anion exchange resin. It showed UV–vis data of $\lambda_{max}(\log \varepsilon) = 423$ (4.82); 490 (3.78); and 598 (3.66) nm in 50 mM PBS at pH 7.4.

Phosphate buffer solutions (PBS, 50 mM) over a wide range of pH were prepared by mixing 50 mM solutions of KOH, KH_2PO_4 and K_2HPO_4 (Wako, analytical grade). The solution pH was monitored using a digital pH meter (TOA, HM-30V). All aqueous solutions were prepared from twice distilled water.

All the solutions were deoxygenated by bubbling ultrapure argon gas (Nippon Sanso, 99.9999%) for 20 min. NO-saturated solution was prepared by bubbling argon and NO mixed gases (Nippon Sanso) into a deoxygenated solution for 30 min before each electrochemical and spectroscopic run. The molar concentration of NO in the solution was evaluated from Ostwald's solubility coefficient [35] for a given partial pressure of NO.

2.2. ITO electrode

Electroconductive indium-tin oxide (ITO) is a very promising material for the characterization of biological systems. The ITO surface is stable under physiological conditions because of its polarizable properties, maintaining a high sensitivity without an insulating oxide layer. Cyclic voltammograms of NO, NO_2^-, and Fe^{III}(4-TMPyP) were measured at an ITO and at a glassy carbon (GC) electrode. The ITO electrode showed lower currents and more positive peak potentials for the oxidations of NO and NO_2^- than those at a GC electrode. On the other hand, the oxidation behavior of Fe^{III}(4-TMPyP) was almost the same for an ITO and a GC electrode. On a GC electrode, however, oxidation of NO_2^- was overlapped with that of Fe^{III}(4-TMPyP). This obscured the participation of high valent iron porphyrins in the oxidations of NO and NO_2^- on a GC electrode. In this sense, large overpotentials for NO and NO_2^- oxidations at hydrophilic ITO electrode led to the clarification of chemical catalysis by high-valent iron porphyrin for NO and NO_2^- oxidations.

A glass plate coated with a 0.1-μm thick ITO film was used as the ITO electrode. Prior to each experiment, the ITO electrode was first sonicated in acetone for 15 min, followed by rinsing with water, ultrasonic cleaning in concentrated NaOH in water + ethanol (1:1) mixed solvent, and rinsing with water again. It was then immersed in $CHCl_3$ for 10 min, and dried.

2.3. Electrochemical and spectroelectrochemical measurements

Electrochemical experiments were performed on a digital universal processing unit (Fuso, HECS 326) connected to a head box (Fuso, HECS 326-1) in one three-electrode cell. The working areas of the optically transparent ITO electrode and a GC electrode were 18.2 mm^2 and 7.1 mm^2, respectively. The Ag|AgCl|3 M NaCl electrode (BAS, RE-5) and a platinum coil were utilized as reference and counter electrodes, respectively.

Spectroelectrochemical measurements were carried out by means of a polarographic analyzer (Yanako, P-1100) and a multi-channel spectrophotometer (Otsuka Electronics, MCPD-1000). An optically transparent thin

layer electrode (OTTLE) cell was constructed by a combination of two ITO-coated glass plates (total area, 900 mm^2), which served as one working electrode. The distance between the two plates was adjusted to ca. 0.2 mm by using a Teflon spacer. This cell was connected to the bottom of a one-compartment cell through a small rectangular hole. All of the measurements were carried out at room temperature.

2.4. Product analysis

In order to clarify the product in the catalytic oxidation cycle of NO by O=Fe^{IV}(4-TMPyP), an electrolysis was carried out in an OTTLE cell containing Fe^{III}(4-TMPyP) solution at +0.85 V. After the UV–vis spectrum indicated that O=Fe^{IV}(4-TMPyP) had been formed completely, different amounts of NO were added to the OTTLE cell in a glove box filled with argon gas. Then, iron porphyrin in the resulting solution, which is an interfering factor in NO_2^-/NO_3^- detection, was first removed by passing the solution through a tiny chromatographic column filled with a cation exchange resin. The amount of nitrite was determined by using the Griess method [25], and nitrate was determined after reduction to nitrite by nitrate reductase (NO_2^-/NO_3^- Assay Kit-C II, Dojindo), respectively. A similar method was applied to product analysis in the catalytic oxidation cycle of NO_2^- by O=Fe^{IV}(4-TMPyP) π-cation radical.

3. Results and discussion

3.1. Stepwise catalytic behavior of oxoiron(IV) 4-TMPyP complexes towards NO and NO_2^- oxidation

Fig. 1(a) shows the cyclic voltammogram (CV) of Fe^{III}(4-TMPyP) in pH 7.4 PBS at an ITO electrode. At pH 7.4 the hydroxy-aqua iron porphyrin, HO–$Fe^{III}(H_2O)$(4-TMPyP), predominates over diaqua or dihydroxy iron porphyrin, since proton equilibria exist with pK_a values of 5.5 and 11.8 [36]. Two separate oxidation peaks are observed for HO–Fe^{III}(4-TMPyP) (ligand H_2O is omitted for simplicity) around +0.85 and +1.15 V, corresponding to the oxidation of the central iron and porphyrin ring, respectively. The CV of pure NO and NO_2^- in pH 7.4 PBS at an ITO electrode is shown in Fig. 1(d). The oxidation peak potential of NO was observed around +1.0 V compared with +0.65 V at a GC electrode. On the other hand, the peak potential of NO_2^- oxidation was not clear and was estimated by subtracting residual currents to be roughly +1.2 ~+1.3 V (+0.8 V at a GC electrode), but the peak currents were small owing to the large overpotentials for the direct oxidation on the ITO electrode. However, a large peak current was observed at the CV of NO_2^- in the presence of Fe^{III}(4-TMPyP) (Fig. 1(b)). By comparing Fig. 1(b) with Figs. 1(a) and (d), it could be concluded that the enhanced current arose from the catalytic oxidation of NO_2^- by Fe^{III}(4-TMPyP). Fig. 1(c) shows the CV of NO and NO_2^- mixture in the presence of Fe^{III}(4-TMPyP). Simultaneously, two enhanced peak currents were observed around the first and second oxidation potentials of Fe^{III}(4-TMPyP), which are shown in the inset of Fig. 1. These results clearly suggest a stepwise catalytic oxidation behavior of NO and NO_2^- oxidation by high-valent iron porphyrins.

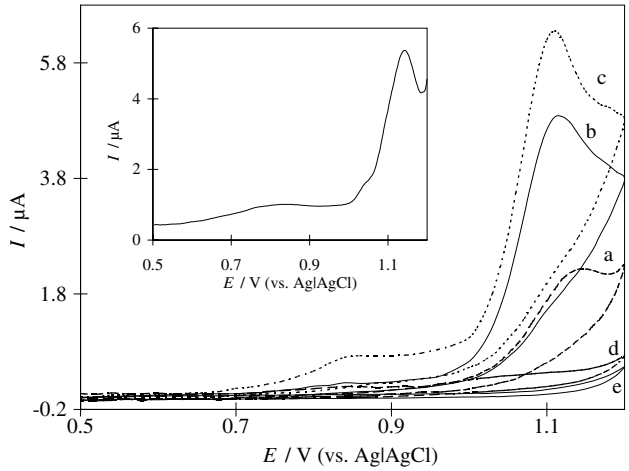

Fig. 1. Cyclic voltammograms of 20 μM Fe^{III}(4-TMPyP) at an ITO electrode in 50 mM pH 7.4 PBS (a) without and (b) with 100 μM NO_2^-, and (c) with 100 μM NO_2^- and 18.3 μM NO. Curves (d) and (e) are obtained in pure PBS with and without 18.3 μM NO and 100 μM NO_2^-, respectively. Scan rate, 10 mV s^{-1}. Inset: differential pulse voltammogram of 20 μM Fe^{III}(4-TMPyP) at an ITO electrode in 50 mM pH 7.4 PBS. Scan rate, 20 mV s^{-1}; pulse amplitude, 25 mV; pulse width, 50 ms.

3.2. Spectroelectrochemical and electrochemical characterization of oxoiron(IV) (4-TMPyP) complexes

It has been reported that oxoiron(IV) species of Fe(4-TMPyP) and some related iron porphyrins exist stably in alkaline solutions at different pH values [37]. However, much of the insight into the oxoiron(IV) porphyrins has been gained from the extensive chemical characterization of these species. To reveal the biological significance, this approach must be complemented by direct measurement under physiological conditions. In this research, electrochemical formation of O=Fe^{IV}(4-TMPyP) during the oxidation of Fe^{III}(4-TMPyP) in pH 7.4 PBS has been confirmed by a spectroelectrochemical method. The further oxidized species, O=Fe^{IV}(4-TMPyP) π-cation radical, has also been estimated to be formed at more positive potential.

Fig. 2 shows the spectral change of Fe^{III}(4-TMPyP) in pH 7.4 PBS at different potentials. Clear isosbestic points were observed at 409, 444, 518 and 572 nm. With

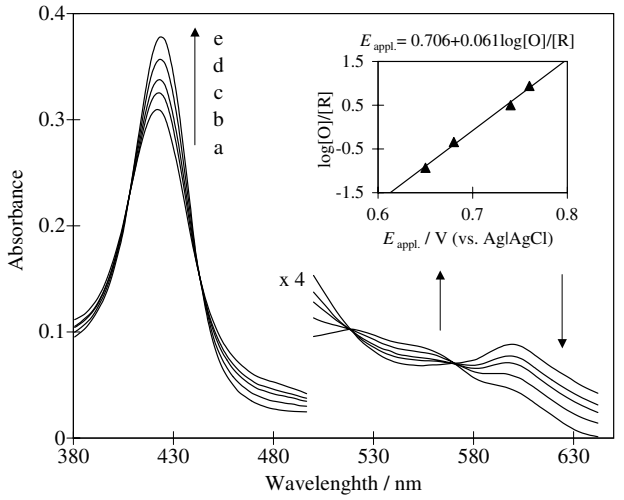

Fig. 2. Typical absorption spectra of Fe^{III}(4-TMPyP) at different potentials in an OTTLE cell which was composed of two ITO-coated glass plates with the optical pathlength of ca. 0.2 mm. (a) At open circuit potential, (b) 0.67, (c) 0.70, (d) 0.74, and (e) 0.76 V. Inset: plot of log[O]/[R] vs. E_{appl}.

increasing applied potential, the Soret band shifted from 423 to 426 nm and the absorbance of the Q band at 598 nm decreased while two new peaks appeared at 517 and 572 nm. The double peaks in the visible region were typical for an intermediate containing an oxoiron(IV) (Fe^{IV}=O) group in Compound II [14]. However, at more positive potential (+1.2 V), the spectra showed a decrease in the absorbance and all peaks disappeared finally.

A plot of log[O]/[R] vs. E_{appl} is shown in the inset of Fig. 2. According to the Nernst equation, the slope of approximately 60 mV/(log[O]/[R]), indicates that the number of electrons transferred in the oxidation of

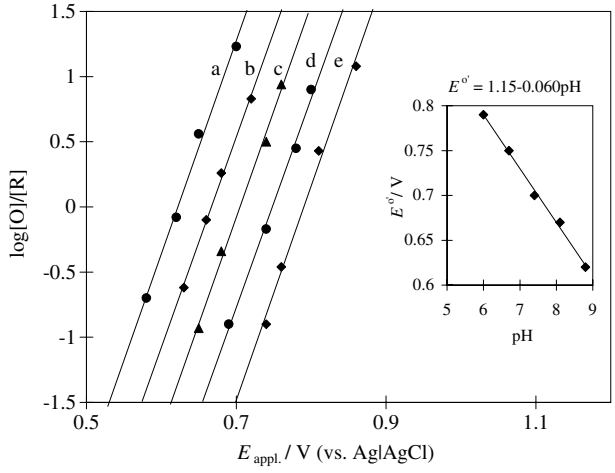

Fig. 3. Plots of log[O]/[R] vs. $E_{appl.}$ in pH (a) 8.8, (b) 8.1, (c) 7.4, (d) 6.7, and (e) 6.0 solution containing 200 μM Fe^{III}(4-TMPyP). [O] = [O=Fe^{IV}(4-TMPyP)], [R] = [Fe^{III}(4-TMPyP)]. Inset: Nernst plot of $E^{0\prime}$ vs. pH.

Fe^{III}(4-TMPyP), n, was 1. The formal potential, $E^{0\prime}$, was +0.706 V (vs. Ag|AgCl) at pH 7.4. Fig. 3 shows the plots of log[O]/[R] vs. E_{appl} at different pHs between 6.0 and 8.8. These plots gave the same slope of 60 mV, and the slope of pH dependence of $E^{0\prime}$ in this pH range was –60 mV/pH. These results indicated that O=Fe^{IV}(4-TMPyP) was formed via a one-electron and one-proton process as shown in the following equation

$$HO\text{–}Fe^{III}(4\text{-TMPyP}) - e^- \rightarrow O{=}Fe^{IV}(4\text{-TMPyP}) + H^+ \quad (1)$$

The fact that H^+ participated in the 1 e^- oxidation of Fe^{III}(4-TMPyP) suggested that the oxidation of HO–Fe^{III}(4-TMPyP) occurred at the metal site, that is, the HO–Fe^{III} site was oxidized to O=Fe^{IV} with the loss of 1 H^+. Since O=Fe^{IV}(4-TMPyP) is confirmed to be stable in pH 7.4 PBS until 1.0 V, Fig. 1(a) shows that O=Fe^{IV}(4-TMPyP) is further oxidized at potentials more positive than +1.0 V. Groves et al. [38] have confirmed that 1 e^- oxidation of oxo-ligated iron(IV) porphyrin preferentially generates an iron(IV) porphyrin π-cation radical rather than an iron(V) porphyrin. Therefore, the second oxidation of HO–Fe^{III}(4-TMPyP) occurs on the porphyrin ring to generate O=Fe^{IV}(4-TMPyP) π-cation radical following the equation

$$O{=}Fe^{IV}(4\text{-TMPyP}) - e^- \rightarrow O{=}Fe(4\text{-TMPyP})^{+\cdot} \quad (2)$$

Close examination of the second oxidation was performed using differential pulse voltammetry (DPV). Two splitting peaks were observed around +1.02 and +1.15 V, which represent the successive oxidation of the porphyrin ring (inset of Fig. 1). The first shoulder peak suggested the formation of O=Fe^{IV}(4-TMPyP) π-cation radical. Further, controlled-potential coulometry (CC) at a thin-layer cell containing Fe^{III}(4-TMPyP) was carried out at fixed potentials of +0.85 and +1.2 V, respectively. According to the Faraday law

$$Q = nFN, \quad (3)$$

where F is Faraday's constant, N is the molar number of Fe^{III}(4-TMPyP) in the cell, Q is the charge during the CC experiment and the number of electrons transferred (n) was approximately 1 at 0.85 V and 4 at 1.2 V, respectively. These results indicated that Fe^{III}(4-TMPyP) was oxidized via one electron oxidation to O=Fe^{IV}(4-TMPyP) and following the second oxidation, generated multiply oxidized species through O=Fe^{IV}(4-TMPyP) π-cation radical. The 1 e^- oxidized species of O=Fe^{IV}(4-TMPyP), O=Fe^{IV}(4-TMPyP) π-cation radical, was stable in aprotic solvent and was confirmed by cyclic voltammetry [17]. However, O=Fe^{IV}(4-TMPyP) π-cation radical in aqueous solution was stable only on the cyclic voltammetric time scale at ambient temperatures and could be further oxidized at the porphyrin ring to form multiply oxidized species [39]. It has been known that the oxidation of porphyrin ring combining with the

nucleophilic attack of hydroxide ion leads to destruction of the macrocycle of porphyrin. Overall, the spectroelectrochemical data suggested the formation of O=Fe^{IV}(4-TMPyP) by the 1 e^- oxidation of Fe^{III}(4-TMPyP) in pH 7.4 and the further oxidation of the porphyrin ring to generate O=Fe^{IV}(4-TMPyP) π-cation radical, followed by multiply oxidized species.

3.3. Catalytic oxidation of NO by O=Fe^{IV}(4-TMPyP)

Fig. 4 shows cyclic voltammograms of NO and Fe^{III}(4-TMPyP) at the ITO electrode in 50 mM pH 7.4 PBS. The direct oxidation current of NO (Fig. 4(d)) was very small at ITO electrode owing to the large overpotential, but the presence of Fe^{III}(4-TMPyP) (Fig. 4(a)) resulted in a significant current increase. A comparison of Fig. 4(a) with Fig. 4(b) indicates that the oxidation of NO proceeds along with the oxidation of Fe^{III}(4-TMPyP). These results suggested one catalytic process of Fe^{III}(4-TMPyP) towards NO oxidation through an EC catalytic regeneration mechanism. A feature of this mechanism was that the iron porphyrin must first be oxidized to O=Fe^{IV}(4-TMPyP) at the ITO electrode. To our knowledge, this is the first report on the catalytic oxidation of NO by oxoiron(IV) porphyrin.

The catalytic oxidation of NO was investigated at various concentrations of Fe^{III}(4-TMPyP). The normalized catalytic current ($I_{p,Nc}$) was calculated according to the equation [40]

$$I_{p,Nc} = (I_{p,cat} - I_{p,M})/I_{p,n=1}, \quad (4)$$

where $I_{p,M}$ is the current contributed by the catalyst itself; $I_{p,n=1}$ is the current for one-electron oxidation of NO calculated from the Randles–Sevčik equation [41].

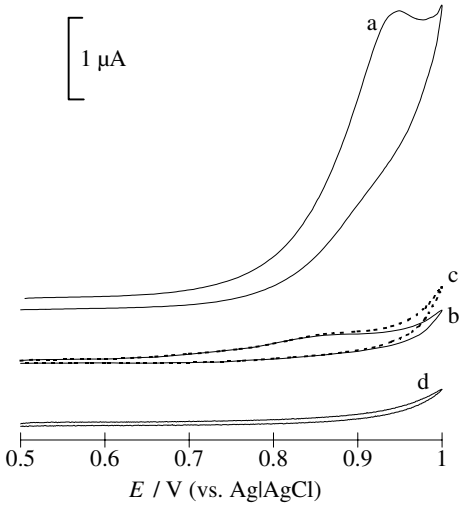

Fig. 4. Cyclic voltammograms of 20 μM Fe^{III}(4-TMPyP) at an ITO electrode in 50 mM PBS (pH 7.4) (a) with and (b) without 82.3 μM NO, and (c) with 20 μM NO_2^-. Curve (d) is obtained in pure PBS with 82.3 μM NO. Scan rate, 10 mV s^{-1}.

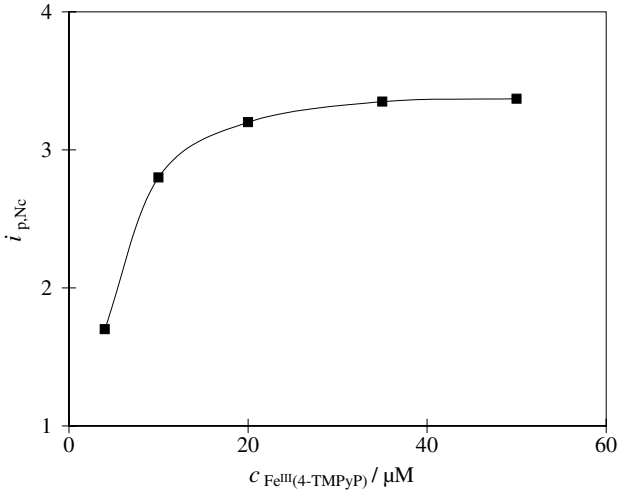

Fig. 5. Plot of the normalized catalytic current vs. Fe^{III}(4-TMPyP) concentration. NO concentration, 82.3 μM; scan rate, 10 mV s^{-1}.

The plot of $I_{p,Nc}$ vs. the concentration of catalyst is exhibited in Fig. 5, $I_{p,Nc}$ increased rapidly with an increasing Fe^{III}(4-TMPyP) concentration up to ca. 0.02 mM and reached a maximum value of 3.4 after a ratio of catalyst/NO of 1:4. Anson [42] suggested that $E_{p,cat}$ would be more negative than the redox potential of catalyst at the high kinetic rate of the reaction. This phenomenon was observed in the present experiment. $E_{p,cat}$ moved to more negative potentials from 0.97 to 0.89 V, as the iron porphyrin concentration increased from 0.004 to 0.05 mM. On the other hand, it was also observed that the catalytic current for NO oxidation increased with an increasing solution pH. These results indicated that the reactions (1) and (5) were very fast

$$\text{O=Fe}^{IV}\text{(4-TMPyP)} + \text{NO} + \text{OH}^- \rightarrow \text{HO–Fe}^{III}\text{(4-TMPyP)} + \text{NO}_2^- \quad (5)$$

Interestingly, an addition of nitrite into Fe^{III}(4-TMPyP) solution caused little change of the cyclic voltammogram in the potential window of +0.5 to +1.0 V (Figs. 4(b) and (c)). Thus, nitrite was not oxidized in that potential range. O=Fe^{IV}(4-TMPyP) showed high selectivity for NO oxidation against NO_2^-.

Fig. 6 shows the reactivity of electrogenerated O=Fe^{IV}(4-TMPyP) with NO and NO_2^-. O=Fe^{IV}(4-TMPyP) was relatively stable in both PBS and PBS containing NO_2^- (Figs. 6(a) and (c)) and was quickly reduced back to Fe^{III}(4-TMPyP) upon addition of NO (Fig. 6(b)). The initial slope of the decay curve corresponded to the reduction rate of O=Fe^{IV}(4-TMPyP). The slope ratio of NO to NO_2^-, which was corrected to the natural decay (Fig. 6(a)), was about 120. This value was almost the same as the estimated free NO concentration ratio of 128 in NO and NO_2^- solutions. NO in

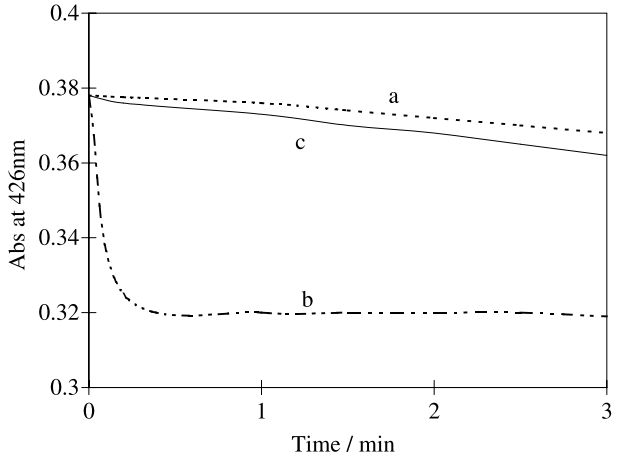

Fig. 6. UV–vis absorbance change at 426 nm monitored for the decay reaction of O=Fe^{IV}(4-TMPyP) to Fe^{III}(4-TMPyP) in 50 mM PBS (a) without and (b) with 82.2 μM NO, and (c) with 100 μM NO_2^-.

NO_2^- was generated thermodynamically according to the disproportionation reaction of NO_2^- [43]

$$2NO_{aq} + NO_3^- + 2OH^- \rightleftharpoons 3NO_2^- + H_2O \quad K = 1.1 \times 10^{20}\ M^{-2} \tag{6}$$

1 mol% nitrite even in pH 7.4 could be disproportionated into nitrate and NO (0.64 mol%). In this sense, O=Fe^{IV}(4-TMPyP) could not be reduced by nitrite.

After a bulk electrolysis of 100 μM Fe^{III}(4-TMPyP) was carried out at +0.85 V for 10 min in PBS, different concentrations of NO were added to the electrolyzed solution. Product analysis exhibited that the absorbance of nitrite by Griess assay [25] at 540 nm was proportional to the amount of NO added, which indicated that the reaction of electrogenerated O=Fe^{IV}(4-TMPyP) with NO led to the formation of nitrite. Therefore, nitrite was the product in the catalytic oxidation of NO by O=Fe^{IV}(4-TMPyP). This result was in good agreement with the result that no catalytic current for NO_2^- oxidation was observed in Fig. 4(c).

As a conclusion, O=Fe^{IV}(4-TMPyP) selectively oxidized NO to form NO_2^- anion. Herold and Rahmann [44] noted the rapid formation of $MbFe^{III}ONO$ intermediate in the reaction between $MbFe^{IV}$=O and NO. The direct incorporation of this oxygen atom into NO, yielding nitrite, may account for the relatively rapid reaction rate, compared with the slow rate of NO binding to ferric porphyrin. On the other hand, no catalytic current of NO oxidation was observed when an electrode was exposed to a Fe^{III}(4-TMPyP) solution for 20 min and then rinsed thoroughly with distilled water, in contrast to the case of strong absorbable catalyst. Thus, these results indicated that the catalytic oxidation cycle of NO by oxoiron (IV) porphyrin was not electrocatalysis but was a typical chemical catalysis via an intermediate to give nitrite as the product [45]. Compared with the direct oxidation on ITO, chemical catalysis (inner-sphere process) showed an increase in the catalytic current. A reaction consistent with the above observations would involve reaction (1) followed by the equations:

$$O{=}Fe^{IV}(4\text{-TMPyP}) + NO \rightarrow ONO{-}Fe^{III}(4\text{-TMPyP}) \tag{7}$$

$$ONO{-}Fe^{III}(4\text{-TMPyP}) + OH^- \rightarrow HO{-}Fe^{III}(4\text{-TMPyP}) + NO_2^- \tag{8}$$

3.4. Catalytic oxidation of NO_2^- by O=Fe(4-TMPyP) π-cation radical

Fig. 7 shows the CVs of Fe^{III}(4-TMPyP) at an ITO electrode in PBS containing nitrite at different concentrations. The peak current around +1.1 V, which corresponded to the catalytic oxidation of nitrite, increased gradually with increasing concentration of nitrite, while the peak potential, $E_{p,cat}$, shifted to more negative value. Such a negative shift of $E_{p,cat}$ suggested the participation of the first oxidized species of O=Fe^{IV}(4-TMPyP), namely O=Fe^{IV}(4-TMPyP) π-cation radical, in the catalytic oxidation of NO_2^-. Fig. 7, curves a and f are the CVs of Fe^{III}(4-TMPyP) and nitrite, respectively. Although the concentration of nitrite was 7.5 times that of Fe^{III}(4-TMPyP), its direct oxidation on the ITO electrode exhibited much smaller oxidation currents, indicating a slow oxidation process. However, in the presence of Fe^{III}(4-TMPyP) the current of NO_2^- oxidation was dramatically increased. This enhanced current

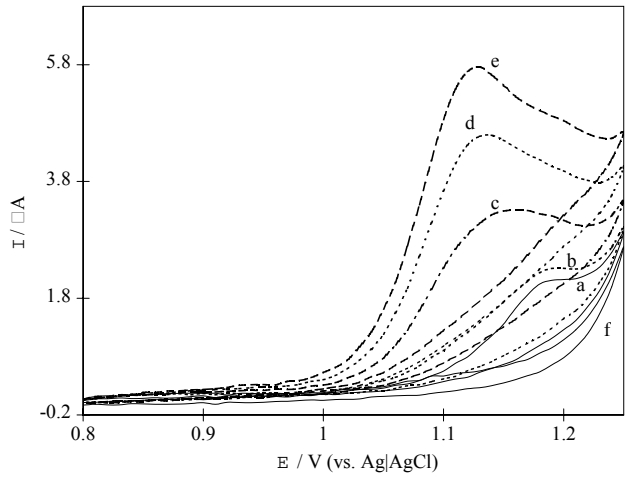

Fig. 7. Cyclic voltammograms of 20 μM Fe^{III}(4-TMPyP) at an ITO electrode in 50 mM pH 7.4 PBS upon successive additions of NO_2^- at the concentrations of (a) 0, (b) 10, (c) 50, (d) 100, and (e) 150 μM. Curve (f) is obtained in PBS containing 150 μM NO_2^-. Scan rate, 10 mV s^{-1}.

was speculated to result from a catalytic cycle of NO_2^- oxidation as shown in the following equations:

$$O{=}Fe^{IV}(4\text{-TMPyP})^{+\cdot}{\cdot}NO_2^- \rightarrow O{=}Fe^{IV}(4\text{-TMPyP}) + {\cdot}NO_2 \quad (9)$$

$$2{\cdot}NO_2 \rightleftharpoons N_2O_4,$$

$$\text{then } N_2O_4 + H_2O \xrightarrow{k_1=7\times10^5\,M^{-1}s^{-1}} NO_2^- + NO_3^- + 2H^+ \quad (10)$$

$$\text{or } O{=}Fe^{IV}(4\text{-TMPyP}) + {\cdot}NO_2 \rightarrow Fe^{III}(4\text{-TMPyP}) + NO_3^- \quad (11)$$

In the first process, O=Fe^{IV}(4-TMPyP) π-cation radical reacted with nitrite to produce O=Fe^{IV}(4-TMPyP) and $\cdot NO_2$. It has been reported that NO_2^- can be oxidized by heme peroxidases such as HRP, MPO, and LPO in the presence of hydrogen peroxide, most likely to generate nitrogen dioxide ($\cdot NO_2$) intermediate [29,30]. There are two possibilities for the fate of $\cdot NO_2$: one is subsequent dimerization of $\cdot NO_2$ to N_2O_4 and followed by hydrolysis to NO_2^- and NO_3^- (Eq. (10)), whose overall rate constant is 7×10^5 M^{-1} s^{-1} [46]; another is that $\cdot NO_2$ is oxidized by O=Fe^{IV}(4-TMPyP) to NO_3^- (Eq. (11)). In fact, the inset of Fig. 8(b) shows that no change in the spectrum of Fe^{III}(4-TMPyP) was observed during the electrolysis at +1.1 V in the presence of nitrite. However, Fe^{III}(4-TMPyP) started its typical oxidation process after NO_2^- was fully consumed. Alternatively, Fe^{III}(4-TMPyP) and nitrate are generated as the final products in the fast reaction between O=Fe^{IV}(4-TMPyP) and $\cdot NO_2$.

Product analysis also exhibited that nitrite could be rapidly oxidized to nitrate by O=Fe^{IV}(4-TMPyP) π-cation radical. When a mixed solution of NO_2^- and Fe^{III}(4-TMPyP) was electrolyzed in an OTTLE cell with an applied potential of +1.1 V, the product analysis showed NO_2^- and NO_3^- coexisting in the resulting solution (Fig. 8). Moreover, the increase of NO_3^- concentration was proportional to the decrease of nitrite concentration. After the electrolysis time when the formation of O=Fe^{IV}(4-TMPyP) π-cation radical was confirmed, the resulting solution showed that all of the NO_2^- are oxidized to NO_3^-. The phenomena suggested that the catalytic oxidation of nitrite to nitrate by O=Fe^{IV}(4-TMPyP) π-cation radical was rapid and quantitative. Shimanovich and Groves [47] showed the reaction between O=Fe(IV)TMPS with $\cdot NO_2$ was a rapid reaction with the rate constant of $k_2 = 1.7 \times 10^7$ M^{-1} s^{-1} by kinetic simulations. When an excess of $\cdot NO_2$ was allowed to react with $MbFe^{IV}$=O, the intermediate complex, $MbFe^{IV}ONO_2$, was generated with an approximate second order rate constant of 1×10^7 M^{-1} s^{-1} [48]. Comparing the kinetic constant $k_1(7 \times 10^5$ M^{-1} $s^{-1})$ with $k_2(1.7 \times 10^7$ M^{-1} $s^{-1})$, the kinetic feasibility further supposed $\cdot NO_2$ was more easily able to react with O=Fe^{IV}(4-TMPyP) than to dimerize. Therefore, the electrogenerated O=Fe^{IV}(4-TMPyP) π-cation radical effectively catalyzed the oxidation of NO_2^- as a two-electron oxidant: NO_2^- anion was first oxidized to NO_2 radical and then interacted with O=Fe^{IV}(4-TMPyP) to give Fe^{III}(4-TMPyP) and nitrate as the final products.

A remarkable feature of the above experiment was the small amount of decomposition of Fe^{III}(4-TMPyP) in the presence of nitrite. The absorbance of the Soret band at 423 nm was almost the same as that in the early stage of experiment. However, in the absence of nitrite, electrolysis for 10 min resulted in 20% decomposition of Fe^{III}(4-TMPyP). It is known that porphyrin ring oxidation causes a nucleophilic attack by hydroxide ion and then the destruction of the porphyrin ring. The stability of Fe^{III}(4-TMPyP) in the presence of nitrite further indicated that nitrite rapidly reduced O=Fe^{IV}(4-TMPyP)π-cation radical to the stable ferric state in the catalytic oxidation of NO_2^-.

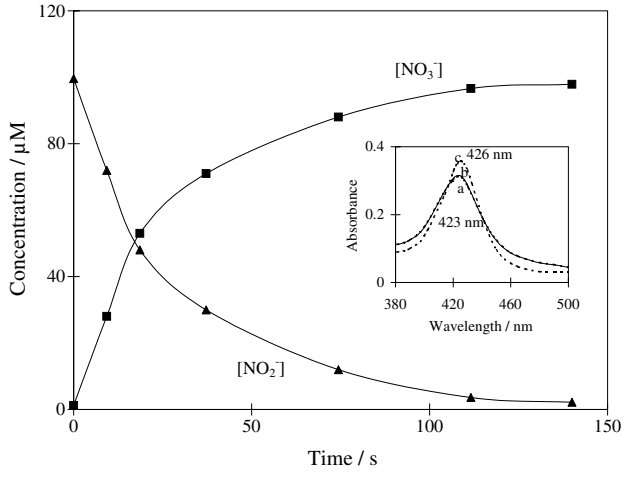

Fig. 8. Plots of NO_2^-(▲) and NO_3^- (■) concentrations vs. electrolytic time in an OTTLE cell containing 200 μM Fe^{III}(4-TMPyP) and 100 μM NO_2^-. Applied potential, +1.1 V. Inset: UV–vis spectra at (a) 0, (b) 130, and (c) 200 s after the application of potential.

4. Conclusion

Oxoiron(IV) porphyrin complexes are potential oxidants in many chemical and biological reactions. This work confirms a stepwise catalytic oxidation of NO and NO_2^- by O=Fe^{IV}(4-TMPyP) and O=Fe^{IV}(4-TMPyP) π-cation radical, respectively. A mechanism has been presented in Scheme 1. NO radical attacks the negatively charged oxygen, interacting with an iron site, and an electron on the oxygen transfers to the Fe^{IV} site by a synchronous process. O=Fe^{IV}(4-TMPyP)exhibits highly selective oxidation for NO against nitrite. The O=Fe^{IV}(4-TMPyP) π-cation radical is a stronger oxidant than O=Fe^{IV}(4-TMPyP) because the redox

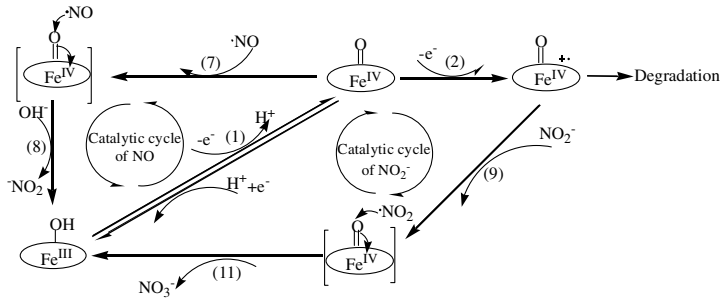

Scheme 1. Proposed reaction mechanism for the catalytic oxidation cycle of NO and NO_2^- by O=Fe^{IV}(4-TMPyP) and O=Fe^{IV}(4-TMPyP) π-cation radical.

potential of the O=Fe^{IV}(4-TMPyP) π-cation radical is higher than that of O=Fe^{IV}(4-TMPyP). The electrogenerated O=Fe^{IV}(4-TMPyP) π-cation radical effectively catalyzes the oxidation of NO_2^- by a two-step process to give nitrate as a final product. This enhanced catalytic current can be utilized to detect NO and NO_2^- in a same time in physiological environments and lead to possible development of highly selective NO and NO_2^- biosensors. On the other hand, the reaction of high-valent iron porphyrin with reactive nitrogen species may represent a detoxifying pathway for both high-valent iron porphyrin and reactive nitrogen species. It is important to further explore the significance of NO and NO_2^- upon Fe^{IV}/Fe^{III} redox couple in biological system.

References

[1] S. Moncada, R.M.J. Palmer, E.A. Higgs, Pharmacol. Rev. 43 (1991) 109.
[2] T. Malinski, Z. Taha, Nature 358 (1992) 676.
[3] S. Kim, G. Deinum, M.T. Gardner, M.A. Marletta, G.T. Babcock, J. Am. Chem. Soc. 118 (1996) 8769.
[4] S. Pfeiffer, B. Mayer, B. Hemmens, Angew. Chem. Int. Ed. 38 (1999) 1714.
[5] M.H. Barley, M.R. Rhodes, T.J. Meyer, Inorg. Chem. 26 (1987) 1746.
[6] S.H. Cheng, Y.O. Su, Inorg. Chem. 33 (1994) 5847.
[7] D. Mimica, J.H. Zagal, F. Bedioui, Electrochem. Commun. 3 (2001) 435.
[8] M. Bayachou, R. Lin, W. Cho, P.J. Farmer, J. Am. Chem. Soc. 120 (1998) 9888.
[9] T. Malinski, M. Kapturczak, J. Dayharsh, D. Bohr, Biochem. Biophys. Res. Commun. 194 (1993) 654.
[10] T. Malinski, F. Bailey, G.Z. Zhang, M. Chopp, J. Cereb. Flow Metab. 13 (1993) 355.
[11] F. Lantoine, S. Trevin, F. Bedioui, J. Devynck, J. Electroanal. Chem. 392 (1995) 85.
[12] M. Pallini, A. Curulli, A. Amine, G. Palleschi, Electroanalysis 10 (1998) 1010.
[13] A.V. Kashevskii, J. Lei, A.Y. Safronov, O. Ikeda, J. Electroanal. Chem. 531 (2002) 71.
[14] P.G. Furtmuller, W. Jantschko, G. Regelsberger, C. Obinger, Biochim. Biophys. Acta 1548 (2001) 121.
[15] Y. Urano, T. Higuchi, M. Hirobe, T. Nagano, J. Am. Chem. Soc. 119 (1997) 12008.
[16] S. Jeon, T.C. Bruice, Inorg. Chem. 31 (1992) 4843.
[17] J.T. Groves, J.A. Gilbert, Inorg. Chem. 25 (1986) 123.
[18] S.M. Chen, Y.O. Su, J. Chem. Soc., Chem. Commun. (1990) 491.
[19] S.E.J. Bell, P.R. Cooke, P. Inchley, D.R. Leanord, J.R.L. Smith, A. Robbins, J. Chem. Soc., Perkin Trans. 2 (1991) 549.
[20] J. Everse, N. Hsia, Free Radic. Biol. Med. 22 (1997) 1075.
[21] F.P. Guengerich, T.L. Macdonald, Acc. Chem. Res. 17 (1984) 9.
[22] J.T. Groves, J. Porph. Phthal. 4 (2000) 350.
[23] Y.M. Goh, W. Nam, Inorg. Chem. 38 (1999) 914.
[24] S.M. Chem, S.W. Chiu, Electrochim. Acta 45 (2000) 4399.
[25] N.V. Gorbunov, A.N. Osipov, B.W. Day, B. Zayas-Rivera, V.E. Kagan, N.M. Elsayed, Biochemistry 34 (1995) 6689.
[26] S. Herold, F.J.K. Rehmann, Free Radic. Biol. Med. 34 (2003) 531.
[27] H.M. Abu-Soud, S.L. Hazen, J. Biol. Chem. 275 (2000) 37524.
[28] H. Fujii, Coord. Chem. Rev. 226 (2002) 51.
[29] H. Shibata, Y. Kono, S. Yamashita, Y. Sawa, H. Ochiai, K. Tanaka, Biochim. Biophys. Acta 1230 (1995) 45.
[30] A.V.D. Viliet, J.P. Eiserich, B. Halliwell, C.E. Cross, J. Biol. Chem. 272 (1997) 7617.
[31] J. Lee, J.A. Hunt, J.T. Groves, J. Am. Chem. Soc. 120 (1998) 7493.
[32] M.P. Jensen, D.P. Riley, Inorg. Chem. 41 (2002) 4788.
[33] R.F. Pasternack, H. Lee, P. Makel, C. Spencer, J. Inorg. Nucl. Chem. 39 (1997) 1865.
[34] F. Bedioui, Y. Bouhier, C. Sorel, J. Devynck, L. Coche-Guerente, A. Deronzier, J.C. Moutet, Electrochim. Acta 38 (1993) 2485.
[35] D.R. Lide (Ed.), CRC Handbook of Chemistry Physics, seventeenth ed., CRC Press, Boca Raton, FL, 1995 (Section 6-3).
[36] N. Kobayashi, M. Koshiyama, T. Osa, T. Kuwana, Inorg. Chem. 22 (1983) 3608.
[37] S.E.J. Bell, R.E. Hester, J.R.L. Smith, in: T.G. Spiro (Ed.), Proceedings of the Fourth International Conference on Time-resolved Vibrational Spectroscopy, Princeton, 1989, pp. 26.
[38] J.T. Groves, R.C. Haushalter, M. Nakamura, T.E. Nemo, B.J. Evans, J. Am. Chem. Soc. 103 (1981) 2884.
[39] T.S. Calderwood, T.C. Bruice, Inorg. Chem. 25 (1986) 3722.
[40] P.A. Forshey, T. Kuwana, Inorg. Chem. 22 (1983) 699.
[41] A.J. Bard, L.R. Faulkner, Electrochemical Methods: Fundamentals and Applications, Wiley, New York, 1980.
[42] F.C. Anson, J. Phys. Chem. 84 (1980) 3336.
[43] D.M. Stanbury, M.M. Demaine, G. Doodloe, J. Am. Chem. Soc. 111 (1989) 5496.
[44] S. Herold, F.K. Rehmann, J. Biol. Inorg. Chem. 6 (2001) 543.
[45] D. Lexa, J.M. Saveant, H.J. Schafer, K.B. Su, B. Vering, D.L. Wang, J. Am. Chem. Soc. 112 (1990) 6162.
[46] J.N. Cape, R.L. Storetonwest, S.F. Devine, R.N. Beatty, A. Murdoch, Atmos. Environ. 27 (1993) 2613.
[47] R. Shimanovich, J.T. Groves, Arch. Biochem. Biophys. 387 (2001) 307.
[48] S. Herold, M. Exner, T. Nauser, Biochemistry 40 (2001) 3385.